The Unusual Catalytic Triad of Poliovirus Protease 3C†

Zsuzsa Sárkány and László Polgár*

Institute of Enzymology, Biological Research Center, Hungarian Academy of Sciences, P.O. Box 7, H-1518 Budapest, Hungary

Received October 15, 2002; Revised Manuscript Received November 18, 2002

ABSTRACT: Picornaviruses are small pathogen RNA viruses, like poliovirus, hepatitis A virus, rhinovirus, and others. They produce a large polyprotein, which is cleaved by virally encoded cysteine peptidases, picornains 2A and 3C. Picornain 3C represents an intermediate between the serine peptidase chymotrypsin and the cysteine peptidase papain. Its steric structure resembles chymotrypsin, but its nucleophile is a thiol instead of the hydroxyl group. The histidine is a general base catalyst in chymotrypsin but forms a thiolate−imidazolium ion pair in papain. The third member of the catalytic triad is an acid (Glu71) as in chymotrypsin rather than an amide found in papain. Transformation of poliovirus 3C peptidase into a serine peptidase results in lower activity by a factor of 430, but the activity extends toward higher pH with the more basic hydroxyl group. The decrease in activity is caused by the less ordered active site, as supported by the unfavorable entropy of activation. At 25 °C the specificity rate constant for the thiol enzyme approaches k_1, the rate constant for the formation of the enzyme−substrate complex, but k_2, the acylation constant, becomes predominant with the increase in temperature. In contrast, for the serine peptidase the specificity constant is less than k_1 over the entire temperature range, and the transition state is controlled by both k_1 and k_2. The acidic component of the catalytic triad is essential for activity, but its negative charge does not influence the ionization of the thiol group.

One of the largest families of human pathogenic RNA viruses is the *Picornaviridae*, which includes poliovirus, hepatitis A virus, rhinovirus, and others. Picornaviruses contain a positive sense strand of RNA, translation of which in infected cells yields a large polyprotein. This polyprotein is cleaved by virally encoded cysteine peptidases, picornains 2A and 3C, to produce mature viral enzymes and structural proteins. Picornain 3C is highly specific for the Gln−Gly bond cleavage (*1*−*5*).

The crystal structures of the 3C peptidases from hepatitis A virus (*6*), rhinovirus (*7*), and poliovirus (*8*) have shown that these enzymes adopt a two-domain β-barrel fold similar to that of chymotrypsin, clearly indicating that the structures of the virus peptidases are basically different from that of the classical cysteine peptidase, papain. The active site geometries of the nucleophilic cysteine side chain and of the general base histidine are virtually superimposable with the equivalent residues, Ser195 and His57, of chymotrypsin (*4*). The shallow active site cleft of PV3C[1] is located at the junction of the two β-barrel domains and contains a catalytic triad composed of His40, Glu71, and Cys147.

Cysteine peptidases are thought to attack the substrate by a thiolate−imidazolium ion pair, as demonstrated with the extensively studied papain. However, we have recently shown that PV3C contains an ordinary thiol group rather than the expected thiolate−imidazolium ion pair (*9*). Therefore, the imidazole assistance in the hydrolysis is very likely general base catalysis, as found with serine peptidases. The structural and mechanistic similarities between picornains and the classic serine peptidases have raised the issue whether a picornain can be converted into an active serine peptidase. This option was not supported by earlier studies, indicating that substitution of serine for the catalytic cysteine residue rendered incapable of processing the polyprotein (*10*, *11*). In contrast, it was demonstrated that some activity was retained with the C147S variant of PV3C, and the modified enzyme exhibited differential effects on the various cleavage sites of the polyprotein (*12*).

Reports on the role of Glu71 of the catalytic triad are also contradictory. On the basis of cleavages of peptides and different fractions of precursor polyprotein, it was concluded that PV3C(E71Q) was proteolytically inactive (*13*). On the other hand, it was found that the Glu71 peptidase had retained some activity (*12*). Processing of the polyprotein is too complex an assay for determining the inherent activity of the mutated enzymes. As quantitative data could not be extracted from such studies, here we report detailed kinetic investigations on the C147S and E71Q variants of PV3C, which allows a deeper insight into mechanistic features of the catalytic triad.

EXPERIMENTAL PROCEDURES

Preparation of PV3C(M27G/C147S). The C147S mutation was introduced into the plasmid pET3d/PV3C(M27G) by the same method as used for the M27G mutation (*9*). The codon TGT for Cys147 was changed to AGT (marked as aGT) for

† This work was supported by the Hungarian Science Fund (OTKA T/9 T022808).

* To whom correspondence should be addressed. Tel: 36-1-279-3110. Fax: 36-1-466-5465. E-mail: polgar@enzim.hu.

[1] Abbreviations: PV3C, poliovirus picornain 3C; PV3C(M27G), Met27Gly variant of poliovirus picornain 3C; PV3C(M27G/C153S), doubly mutated poliovirus picornain 3C; EDTA, ethylenediaminetetraacetic acid; Mes, 2-(morpholino)ethanesulfonic acid; Abz, 2-aminobenzoic acid; DTE, dithioerythritol; Phe(NO_2), 4-nitrophenylalanine.

10.1021/bi027004w CCC: $25.00
Published on Web 12/17/2002

Ser, and a base A was also changed to T (marked in the sense primer as t) to eliminate the *Hin*fI restriction site in the mutated gene, which rendered it possible to verify the mutation. For introduction of the C147S mutation, the following primers were synthesized: sense primer, 5′-GCAGGACAGaGTGGTGGtGTCATCAC-3′; antisense, 5′-GTGATGACaCCACCACtCTGTCCTGC-3′.

From the resulting pET3d/PV3C(M27G/C147S) construction the gene of PV3C(M27G/C147S) was isolated by the two-step PCR method (*9*), using the original primer (5′-CAGAACCATGGGGCCAGGGTTCGA-3′) (*9*) to the 5′-end of the gene with a *Nco*I restriction site (underlined) and a new primer (5′-AGTTTCTCGAGTTGACTCTGAGTGAA-3′) to the 3′-end with an *Avr*II restriction site (underlined) instead of *Bam*HI used in the original 3′ primer. The amplified gene was digested with *Nco*I and *Avr*II restriction endonucleases in the same mixture and ligated into the pET22b(+) vector in frame with the 6 × His tag of the vector. The pET22b(+) vector carries an N-terminal *pelB* signal sequence for potential periplasmic localization. This sequence was excised from the construction pET22b(+)/PV3C(M27G/C147S) by digestion with *Nde*I and *Nco*I restriction endonucleases, which produced overhangs. The DNA polymerase I large (Klenow) fragment was used to generate blunt ends from the 3′-overhangs and T4 DNA ligase for ligation of the blunt ends. The resulting vector contained the PV3C(M27G/C147S) gene without the *pelB* signal. The same procedure was also applied for coupling the 6 × His tag to the parent PV3C(M27G) gene.

The PV3C(M27G/C147S) gene was expressed in *Escherichia coli* BL21(DE3)-pLysE cells. The cells were grown at 37 °C to an OD of 0.5−0.6 at 600 nm in four 2000 mL flasks, each containing 500 mL of LB. Isopropyl β-D-thiogalactopyranoside (0.4 mM) and 50 μg/mL ampicillin were added, and the incubation was continued at 25 °C for about 15 h. The cells were harvested and suspended in 100 mL of binding buffer [20 mM Tris-HCl, pH 7.9, 0.5 M NaCl, 5 mM imidazole, and 1 mM 2-mercaptoethanol (BB)]. The suspension was sonicated on ice and centrifuged for 30 min at 20000*g*. The supernatant was loaded onto a Ni^{2+} chelation column (10 mL), Ni−NTA superflow (QIAGEN). The column was first washed with one column volume of BB and subsequently with one column volume of 20 mM Tris-HCl, pH 7.9, containing 0.5 M NaCl and 10 mM imidazole. The enzyme was eluted with 20 mM Tris-HCl, pH 7.9, containing 0.5 M NaCl and 50 mM imidazole, and concentrated by ultrafiltration on an Amicon PM 10 membrane. During concentration the enzyme was washed with a buffer containing 50 mM Tris-HCl, 0.1 M NaCl, 1 mM 2-mercaptoethanol, and 1 mM EDTA. From 2000 mL of broth, 50 mg of pure PV3C(M27G/C147S) was obtained. The enzyme exhibited a k_{cat}/K_m of 3.75 M^{-1} s^{-1} measured at pH 8.0.

The E71Q mutation was introduced into the plasmid pET3d/PV3C(M27G/C153S) (*9*) by the same method as used for the C147S mutation. The codon GAA of Glu71 was changed to CAG for Gln, and a base T was changed to G in order to create a *Pst*I restriction site (underlined). This allowed us to verify the mutation by digestion. For introduction of the E71Q mutation, the following primers were synthesized: sense primer, 5′-GGAACCAATCTgcAgATCACTATAATC-3′; antisense, 5′-GATTATAGTGATCTgcAGATTGGTTCC-3′.

From pET3d/PV3C(M27G/C153S/E71Q) the gene of PV3C(M27G/C153S/E71Q) was isolated and ligated into the pET22b(+) vector in frame with the 6 × His tag of the vector by the same method described above for PV3C(M27G/C147S). The *pelB* signal sequence was also excised from pET22b(+)/PV3C(M27G/C153S/E71Q).

The enzyme was expressed and purified as described for PV3C(M27G/C147S). From 2000 mL of broth, 37.0 mg of pure PV3C(M27G/C153S/E71Q) was obtained.

Kinetic Measurements. The activity of PV3C(M27G/C147S) was measured fluorometrically with the internally quenched substrate Abz-Glu-Ala-Leu-Phe-Gln-Gly-Pro-Phe-(NO_2)-Ala that is cleaved at the Gln−Gly bond. A sample (0.3 μL) of the substrate stock solution (1 mg/mL in dimethylformamide) was added to the reaction mixture of 1.0 mL final volume containing 40 mM Tris-HCl, pH 8.0, 1 mM EDTA, and 1 mM DTE. Pseudo-first-order rate constants were determined at 25 °C using a Cary Eclipse fluoroscence spectrophotometer equipped with a Peltier four-position multicell holder and a temperature controller. The excitation and emission wavelengths were 330 and 420 nm, respectively. The second-order rate constant (k_{cat}/K_m) was calculated by dividing the pseudo-first-order rate constant by the enzyme concentration. The enzyme concentration was calculated from the absorbance at 280 nm by using M_r value of 20000 and A_{280} (0.1%) of 0.42 (*14*). Active site titration of picornain 3C was carried out as described (*9*).

The pH dependence of the rate constants was measured at 25 °C in a buffer containing 25 mM acetic acid, 25 mM Mes, 25 mM glycine, 75 mM Tris-HCl, and 1 mM EDTA (standard buffer), adjusted to the required pH by the addition of 1 M NaOH or 1 M HCl. The data were fitted by nonlinear regression analysis, using eq 1 and the GraFit software (*15*):

$$k = k(\text{limit})[1/(1 + 10^{pK_1 - pH} + 10^{pH - pK_2})] \qquad (1)$$

where k(limit) is the pH-independent rate constant and pK_1 and pK_2 stand for the pK_a values of catalytically competent functional groups.

The molar extinction coefficient of the dissociated thiol group in PV3C(M27G/C153S/E71Q) was determined at 250 nm by monitoring the absorbance change during alkylation as described in detail (*16*). Samples of 12.4−20.5 μM PV3C(M27G/C153S/E71Q) were alkylated with 0.79 mM iodoacetate in a buffer composed of 25 mM acetic acid, 25 mM Mes, 25 mM glycine, 75 mM Tris-HCl, and 0.2 mM EDTA at 25 °C.

Rate-limiting general base/acid catalysis was tested in heavy water (99.9%). The deuterium oxide content of every reaction mixture was at least 98%. The p^2H of deuterium oxide solutions can be obtained from pH meter readings according to the relationship p^2H = pH(meter reading) + 0.4 (*17*).

The temperature dependence of the rate constants was determined at appropriate temperatures using a Peltier four-position multicell holder. The reactions were started after the thermal equilibrium had been reached in the cell, which was equipped with the temperature controller. Activation parameters were calculated from the linear plots of $\ln(k/T)$ versus $1/T$:

$$\ln(k/T) = \ln(R/N_A h) + \Delta S^*/R - \Delta H^*/RT \qquad (2)$$

Table 1: Kinetic Parameters for PV3C Variants

variant	k_{cat}/K_m(limit)	pK_1	pK_2
M27G/C147S ($M^{-1}\,s^{-1}$)	3.96 ± 0.06	6.60 ± 0.03	9.67 ± 0.04
M27G ($mM^{-1}\,s^{-1}$)[a]	2.55 ± 0.04	6.17 ± 0.05	8.52 ± 0.05

[a] From ref *9*.

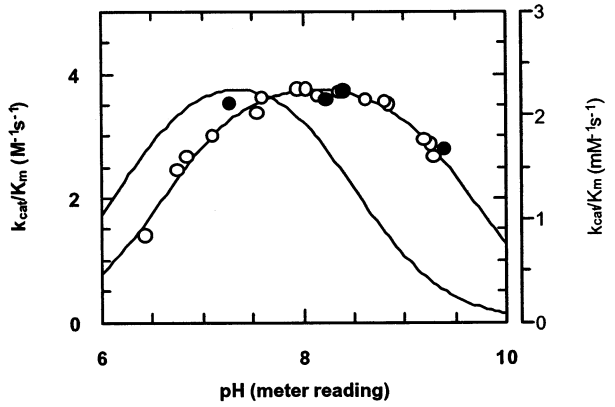

FIGURE 1: The pH−rate profiles for the PV3C(M27G/C147S). The reactions were measured with Abz-Glu-Ala-Leu-Phe-Gln-Gly-Pro-Phe(NO_2)-Ala in standard buffer (○, left ordinate) and in deuterium oxide (●, left ordinate). As a comparison, the pH−k_{cat}/K_m profile for PV3C(M27G) is shown by a thin line (right ordinate) from ref *9*.

where k is an apparent first-order rate constant calculated for the reaction with 1.0 M enzyme, R is the gas constant (8.314 J·mol^{-1}·K^{-1}), T is the absolute temperature, N_A is the Avogadro number, h is the Planck constant, the enthalpy of activation $\Delta H^* = -(\text{slope}) \times 8.314$ J·mol^{-1}, and the entropy of activation $\Delta S^* = (\text{intercept} - 23.76) \times 8.314$ J·mol^{-1}·K^{-1}. The free energy of activation, ΔG^*, was calculated from the equation:

$$\Delta G^* = \Delta H^* - T\Delta S^* \quad (3)$$

RESULTS AND DISCUSSION

The PV3C gene contains an inner initiation codon ATG for Met27, which is responsible for the production of a substantial amount of truncated protein (*18*). Therefore, we have used the PV3C(M27G) variant that proved to be indistinguishable from the wild-type enzyme by activity measurements (*9*). This enzyme was employed for the preparation of the PV3C variants.

pH Dependence of the Reaction of PV3C(M27G/C147S). The replacement of the catalytic cysteine of PV3C by a serine residue results in a 430-fold reduction in the specificity rate constant (Table 1). The pH−rate profiles for the two enzymes are also different (Figure 1). The bell-shaped curve for the modified enzyme is shifted toward the alkaline pH values by 0.45 unit on the acidic side and by 0.9 unit on the alkaline side (Table 1), while the hydrolysis products of the two enzymes are identical, as determined with HPLC. The reduction in the rate constant for the enzyme variant at high pH is not the consequence of protein denaturation since the modified enzyme maintains its catalytic activity upon incubation at pH 9.5 for 1 h. The enzyme is also stable at pH 9.5 when determined by differential scanning calorimetry (Table 2). Interestingly, the stability of the enzyme increases at high pH. The decrease at high pH in the activity of the thiol enzyme very likely arises from the dissociation of the thiol group. Above pH 8.5 the thiol group loses its proton that is essential for the general base and the subsequent general acid catalyses. This proton is a catalytically competent species, which must be transferred to the imidazole in order that the resulting imidazolium ion, as a general acid, should be able to protonate the leaving group of the tetrahedral intermediate. The same mechanism holds with serine peptidases (cf. ref *19*), but the pK_a of the serine OH group is much higher than that of the thiol group, so that the OH group does not lose its proton in the pH range studied. Therefore, the decrease in activity may be due to conformational changes, such as observed with the chymotrypsin reactions (*19*). Indeed, the stability of the enzyme significantly changes at high pH (Table 2), which may be associated with the alteration in the state of ionization of some lysine residues.

Table 2: Melting Points of PV3C Variants

variant	pH 8.0	pH 8.5	pH 9.5
M27G/C147S (°C)	46.5	47.7	50.4
M27G (°C)	46.7	48.1	50.0

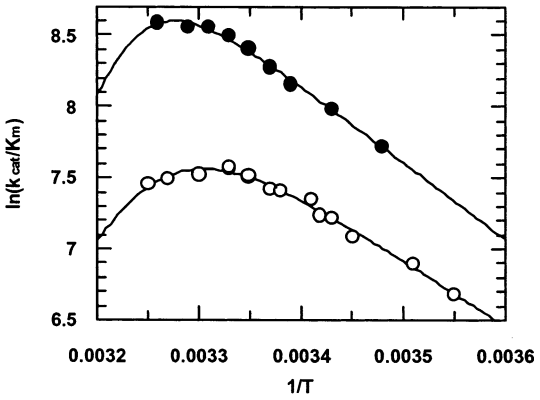

FIGURE 2: Arrhenius plots for PV3C(M27G). The specificity rate constants were measured at the pH optimum (7.6) with 4.77 μM enzyme in H_2O (○) and ^2H_2O (●).

The low-pH limb of the pH−rate profile is associated with the dissociation of the catalytic histidine. The simplest explanation of the pK_a shift for the enzyme variant may be the altered environment of the imidazole group, influenced mainly by the oxygen in place of the sulfur atom. In this environment the imidazole is better protonated, and this may lead to an increase in the pK_a value.

Temperature Dependence. We have previously shown that the Eyring plot [$1/T$ vs $\ln(k/T)$] for PV3C(M27G) deviates from the linear dependence both in H_2O and in ^2H_2O (*9*). The maximum activity (Figure 2) with the thiol enzyme had been reached before the protein tended to denature with the increase in temperature. Indeed, the enzyme retained full activity at 25 °C after incubation at the highest temperature employed.

Low-temperature optimum, such as found with the PV3C-(M27G), is uncommon among enzyme reactions. A similar temperature effect was observed with thrombin, and the phenomenon was interpreted in terms of the change in the

Table 3: Kinetic Parameters for PV3C(M27G)

parameter	10 °C	15 °C	20 °C	25 °C	30 °C	35 °C
H_2O						
k_1 ($M^{-1}\,s^{-1}$)	873 ± 18	1162 ± 23	1527 ± 54	1988 ± 108	2563 ± 187	3290 ± 306
k_2/k_{-1}	328 ± 392	94 ± 91	29 ± 21	9.1 ± 4.9	3.0 ± 1.0	1.00 ± 0.17
E_1 (kJ/mol)	38 ± 3	38 ± 3	38 ± 3	38 ± 3	38 ± 3	38 ± 3
$E_{-1} - E_2$ (kJ/mol)	168 ± 30	168 ± 30	168 ± 31	168 ± 31	168 ± 31	168 ± 31
^2H_2O						
k_1 ($M^{-1}\,s^{-1}$)	1697 ± 66	2362 ± 45	3240 ± 59	4396 ± 159	5903 ± 333	7881 ± 607
k_2/k_{-1}	7114 ± 21207	1184 ± 2834	217 ± 367	41 ± 47	8 ± 5	1.7 ± 0.3
E_1 (kJ/mol)	45 ± 3	45 ± 3	45 ± 3	45 ± 3	45 ± 3	45 ± 3
$E_{-1} - E_2$ (kJ/mol)	241 ± 84	241 ± 84	241 ± 84	241 ± 83	241 ± 84	241 ± 83

individual rate constants that compose k_{cat}/K_m as defined by the equations (*20*, *21*):

$$E + S \underset{k_{-1}}{\overset{k_1}{\rightleftharpoons}} ES \xrightarrow{k_2} EA \quad (4)$$

$$k_{cat}/K_m = k_1k_2/(k_{-1} + k_2) = k_1\alpha/(1 + \alpha) \quad (5)$$

where k_1 and k_{-1} are the rate constants for binding and dissociation of the substrate, respectively, k_2 is the first-order acylation rate constant, EA is the acyl enzyme, and α represents k_2/k_{-1}, the stickiness of the substrate (*22*). Stickiness is high if $k_{-1} \ll k_2$. It follows from eq 5 that k_{cat}/K_m approximates k_1 whenever $\alpha \gg 1$. The temperature dependence of the rate constants can be obtained from the equation (*20*):

$$k_{cat}/K_m = k_{1,0}\exp[(-E_1/R)(1/T - 1/T_0)]q/(1 + q) \quad (6)$$

where $q = \alpha_0 \exp[E_\alpha/R(1/T - 1/T_0)]$, $k_{1,0}$ is the value of k_1 at the reference temperature $T_0 = 298.15$ K, E_1 is the activation energy associated with k_1, and $E_\alpha = E_{-1} - E_2$. From the temperature dependence of $\ln(k_{cat}/K_m)$ (Figure 2), the value of k_1 and the ratio of k_2/k_{-1} can be obtained together with the corresponding activation energies. As T_0 can be set to any value, the parameters can be calculated for various temperatures. The data obtained in such a way are shown in Table 3.

It can be seen from Table 3 that the ratio of k_2/k_{-1} decreases with the increase in temperature, indicating considerable rate enhancement for the dissociation of the enzyme−substrate complex compared to its conversion into acyl enzyme. While the changes in the reaction are clear, the values display very large errors, in particular at low temperature where $k_2 \gg k_{-1}$, and k_{cat}/K_m approaches k_1. As the substrate dissociation has high activation energy, k_{-1} becomes predominant at high temperature. Thus, a plot of $\ln(k_{cat}/K_m)$ vs $1/T$ yields a distinct maximum curve defined by eq 6 (*20*). Consistent with the assumption made in the Arrhenius law, the activation energies do not alter in a reasonable temperature range. E_α is rather large, indicating a major difference between the activation energies for the dissociation and the breakdown of the enzyme−substrate complex to acyl enzyme.

In contrast to PV3C(M27G), the reaction of the C147S variant follows linear temperature dependence, as illustrated by the Eyring plot, $1/T$ vs $\ln[(k_{cat}/K_m)/T]$, shown in Figure 3A. Therefore, individual rate constants for the C147S variant cannot be calculated. It is the value of k_2 that is expected to decrease in the reaction of the serine enzyme. Hence, k_2 may be smaller than k_{-1} in the entire temperature range, resulting

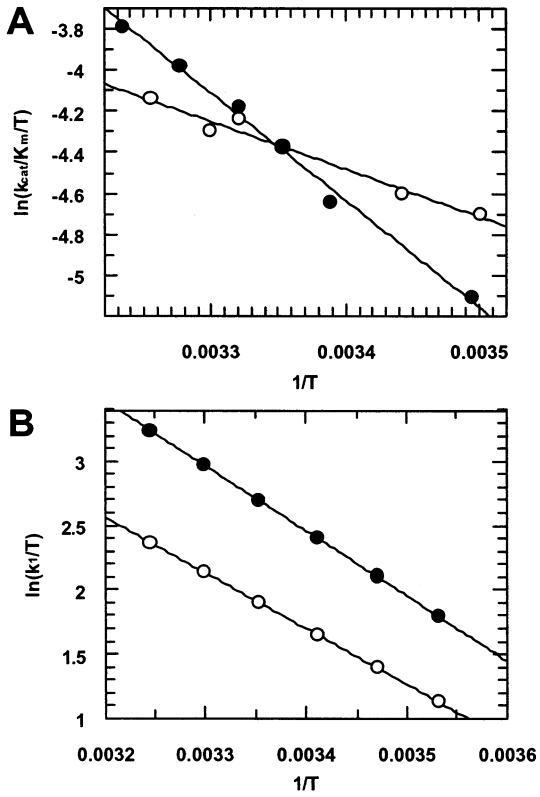

FIGURE 3: Eyring plots for picornain 3C. (A) The reactions measured at pH 8.1 with 34 μM PV3C(M27G/C147S) are represented by k_{cat}/K_m in H_2O (○) and ^2H_2O (●). (B) The k_1 values for the reactions of PV3C(M27G) measured in H_2O (○) and ^2H_2O (●) are taken from Table 3.

in smaller k_{cat}/K_m with respect to k_1. A mechanistic difference between the serine variant and its parent thiol enzyme is that k_2 and k_{-1} approach one another in the thiol enzyme with the increase in temperature, whereas k_2 for the serine enzyme remains smaller than k_{-1} over the available temperature range.

In the thiol enzyme reaction the substrate is a sticky species; i.e., once it is bound, it never leaves the enzyme but is converted into products. In other words, the commitment to catalysis is unity. In the case of the serine enzyme, k_{-1} increases in comparison to k_2, the commitment decreases, and the substrate becomes less sticky.

Solvent Isotope Effects. A further difference between the serine and thiol enzymes concerns the rate-limiting steps of the reactions, which were tested by kinetic deuterium isotope effects at different temperature values. Kinetic deuterium isotope effects have been widely studied to reveal general base-catalyzed processes, which are slower in deuterium

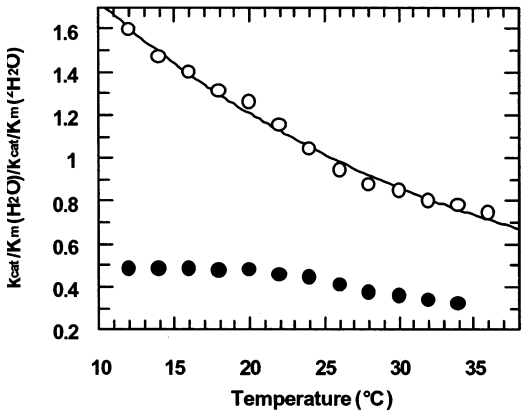

FIGURE 4: Temperature dependence of $k_{cat}/K_m(H_2O)/k_{cat}/K_m(^2H_2O)$. The isotope effects are shown for PV3C(M27G/C147S) (○) and PV3C(M27G) (●).

oxide than in water by a factor of 2−3, as observed in serine protease catalysis, for example, in the chymotrypsin and subtilisin reactions (cf. ref *19*). In contrast to the values characteristic of general base catalysis, picornain 3C exhibited a large inverse effect, $k_{cat}/K_m(H_2O)/k_{cat}/K_m(^2H_2O) = 0.41$. This may be due to conformational changes upon substrate binding and/or structure stabilization in heavy water that promotes catalysis (*9*). This is consistent with the three-dimensional structure of PV3C, indicating that the polypeptide loop preceding Cys147 is flexible and likely undergoes a conformational change upon substrate binding (*8*). An additional concept that can account for the inverse effect is the low fractionation factor of a thiol group ($\phi = 0.41-0.46$) (*23*). The fractionation factor of an exchangeable hydrogenic site is the ratio of protium to deuterium in a mixture of H_2O and ^2H_2O of atom fraction deuterium 0.500. Deuterium accumulates at the more weakly bonded sites, like a thiol group. The fractionation factors of the most common exchangeable sites (OH and NH) are close to unity (*23*). When going from the ground state to the transition state, the fractionation factor of 0.4 changes to 1.0.

In the case of PV3C(M27G/C147S) no kinetic isotope effects were found. As seen in Figure 1, the rate constants determined in water and heavy water fit to the same bell-shaped curve measured at 25 °C. This suggests that the formation of the enzyme−substrate complex, rather than the general base-catalyzed chemical acylation, is predominant in the rate-determining step.

With the thiol enzyme the inverse effect is maintained over the whole temperature range (Figure 4) with only a slight change with temperature. In contrast, with the serine enzyme the kinetic isotope effect decreases exponentially from normal to inverse, displaying no isotope effect at 25 °C (Figure 4). As discussed above, in the case of the thiol enzyme there is a full commitment to catalysis. The formation of the enzyme−substrate complex predominates the reaction ($k_{cat}/K_m \sim k_1$), which is associated with a large inverse effect. With the serine enzyme normal isotope effects are apparent at low temperature, indicating that the k_2 is expressed in the transition state. This implies that the reaction has a virtual (*23*) or composite transition state, involving both the formation of the enzyme−substrate complex and acylation [$k_{cat}/K_m = k_1k_2/(k_{-1} + k_2)$]. The contribution of acylation to the rate-limiting transition state significantly depends on the temperature.

Table 4: Thermodynamic Parameters for PV3C Variants[a]

variant	ΔH^* (kJ·mol^{-1})	ΔS^* (J·mol^{-1}·K^{-1})	ΔG^* (kJ·mol^{-1})
M27G/C147S	19.2	−170	69.8
M27G/C147S (^2H_2O)	43.2	−89	69.8
M27G[b]	31.5	−77	54.4
M27G[c] (k_1 in H_2O)	36.0	−61	54.2
M27G[c] (k_1 in ^2H_2O)	42.0	−34	52.2

[a] Measured at the pH optima. [b] Refers to k_{cat}/K_m from ref *9*. [c] Calculated for the rate constant of formation of the enzyme−substrate complex (k_1).

Estimation of Thermodynamic Parameters from Nonlinear Eyring Plots. It can be anticipated that the smaller k_1 in water pertains to higher E_1 and that the higher k_1 in deuterium oxide has a lower E_1. The opposite finding (Table 3), however, indicates that considerable entropy effects should be associated with the reactions in water.

The activation enthalpies (ΔH^*) and entropies (ΔS^*) were calculated from Eyring plots. As the points for k_{cat}/K_m progressively declined from a straight line, the k_1 values for different temperatures were calculated from eq 6, using several different T_0 temperature values, instead of the standard $T_0 = 298.15$ K. The Eyring plots were perfectly linear with the k_1 data (Figure 3B). The thermodynamic parameters extracted from the plots are compiled in Table 4, which also contains the corresponding data for the C147S variant. In the latter case k_{cat}/K_m is used, which does not simplify to k_1 but remains equal to $k_1k_2/(k_{-1} + k_2)$.

The thermodynamic data offer an explanation for the lower activity of the serine enzyme. The radius of the oxygen atom is smaller by 0.4 Å than that of the sulfur atom. Therefore, the reactants must move toward each other within the complex for reaction to occur (entropic effect). The larger sulfur, on the other hand, is able to make a close contact with both the imidazole and the substrate carbonyl carbon atom. This rationale is clearly supported by the large difference in the ΔS^* values for the serine and cysteine peptidases (Table 4). In the case of the serine enzyme the large negative ΔS^* is consistent with a disordered active site that displays enhanced motility, which must be frozen out on going to the transition state. Thus a high entropy barrier can predominantly account for the impaired catalytic efficiency of the modified enzyme.

Effect of Cysteine−Serine Exchange on Substrate Specificity of PV3C. It was reported that the mutants of PV3C, including the C147S variant, have differential effects on the cleavage at different Glu−Gly junctions of the polyprotein (*12*). Among the eight junctions cleaved by PV3C, the peptide comprising the 2C/3A junction is the best substrate (*24*, *25*). The fluorescent derivative of this peptide has been used in this study. To examine a possible change in the specificity of the serine enzyme, we have synthesized a peptide containing the 3C/3D junction: Abz-Phe-Thr-Gln-Ser-Glu-Gly-Glu-Phe(NO_2)-Ala. This proved to be a rather poor substrate (3.75 M^{-1} s^{-1}) compared with that normally used here (2230 M^{-1} s^{-1}). Table 5 shows that the relative decrease in activity is not very different for the two substrates; i.e., the transformation of the thiol peptidase into a serine enzyme does not appreciably modify the specificity.

Importance of Glu71. The classical cysteine peptidases of the papain family contain a neutral asparagine as part of the

Table 5: Effects of Ser147 on the Specificity of PV3C[a]

	initial rate (%)	
enzyme	2C/3A	3C/3D
PV3C(M27G)	100	100
PV3C(M27G/C147S)	0.18	0.28

[a] Specific substrate involving 2C/3A junction: Abz-Glu-Ala-Leu-Phe-Gln-Gly-Pro-Phe(NO_2)-Ala. Poor substrate involving 3C/3D junction: Abz-Phe-Thr-Gln-Ser-Glu-Gly-Glu-Phe(NO_2)-Ala.

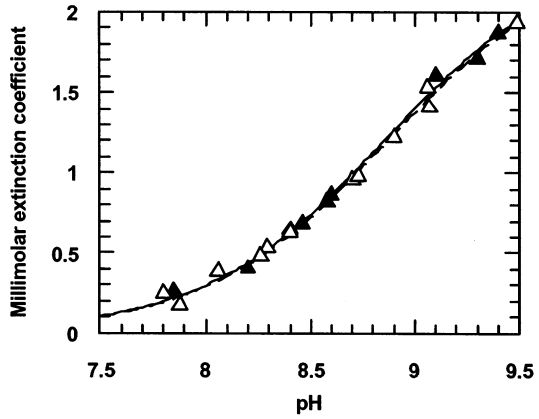

FIGURE 5: pH dependence of the molar extinction coefficient of Cys147. Data for PV3C(M27G/C153S/E71Q) were calculated from alkylation with iodoacetate (▲). The points were fitted to a simple sigmoid curve, using the following parameters: $\epsilon = 2.38 \pm 0.06$ mM^{-1} cm^{-1}; $pK_a = 8.85 \pm 0.03$. The change in the molar extinction coefficient for PV3C(M27G/C153S) is also shown (△, dashed line) from ref *9*. The dashed line practically merges into the solid line.

catalytic triad, whereas the picornains have an aspartic or glutamic acid. This might suggest that, in contrast to serine peptidases, the negative charge is not important at the active site of cysteine peptidases. To study the role of Glu71 of PV3C(M27G/C153S), the charged residue was replaced by the neutral glutamine. For this study the enzyme with a C153S mutation was employed because the elimination of the second cysteine of PV3C facilitated the investigations on the catalytic cysteine residue (see below). Since PV3C-(M27G/C153S/E71Q) proved to be a practically inactive enzyme, a 6 × His tag was added to the C-terminus of the enzyme to facilitate isolation. The extra histidine residues linked to the parent active enzyme did not affect the catalytic activity. The enzyme with Gln71 displayed very low activity, which did not permit the determination of k_{cat}/K_m. However, initial rate measurements could clearly show that the introduction of the mutation decreased the activity by a factor of 40300. Since the thiol group of the enzyme may be more or less oxidized during preparation with partial loss of activity, we have titrated the free thiol groups by the Ellman reagent [5,5′-dithiobis(2-nitrobenzoic acid)] (*26*). Thanks to the single thiol group in PV3C(M27G/C153S/E71Q), the active site thiol group could readily be titrated, and this yielded 0.98 mol of thiol group per mole of enzyme.

The active site of papain involves a thiolate−imidazolium ion pair. In contrast, PV3C has a normal thiol group with a pK_a of 8.86 (*9*). The dissociated form of a thiol group can be detected by alkylation, as this abolishes most of the absorbance of the thiolate ion at 250 nm (*16*). Figure 5 shows that the substitution of Glu71 by a glutamine does not influence the ionization state of the catalytic cysteine, indicating that the nucleophilic reactivity of the thiol group did not alter. Hence, the dramatic reduction in the catalytic activity is very likely due to improper participation of the histidine residue. The crystal structure of PV3C (*8*) shows that the conformation of the imidazole ring is stabilized by a hydrogen bond formed between one of the oxygen atoms of the carboxyl group of Glu71 and $N^{\delta 1}$ of His40. The glutamic acid is further stabilized by hydrogen bonds from His40 N and Asn69 $N^{\delta 2}$ to Glu71 $O^{\epsilon 1}$ and $O^{\epsilon 2}$, respectively. The stabilization of the imidazole ring apparently becomes less effective when the carboxyl oxygen of Glu71 is replaced by the NH_2 group. Accordingly, an intimate interaction between the thiol and imidazole groups, which could modify the pK_a of the thiol group, does not exist, in agreement with the lack of the thiolate−imidazolium ion pair.

Conclusion. The conversion of the nucleophile, Cys147, of PV3C into Ser147 results in an active serine peptidase but with specificity rate constant decreased 430-fold. Owing to the higher pK_a of the hydroxyl group, the modified enzyme remains active at higher pH than the parent thiol enzyme. The reduced activity of the enzyme variant is primarily due to the less ordered ground state of its reaction, as indicated by the large negative entropy of activation.

The mechanisms of action of picornain 3C and its serine variant are different in several respects. At 25 °C the k_{cat}/K_m for the thiol enzyme is close to k_1 but changes with the increase in temperature, as k_2 becomes more and more important, leading to an optimum temperature. For the serine peptidase $k_{cat}/K_m < k_1$, and the transition state involves contributions from both acylation and the formation of the enzyme−substrate complex. Due to the increasing rate limitation by acylation, the inverse isotope effect turns to normal in the lower temperature range.

Glu71 plays a crucial role in the catalysis, as its replacement by glutamine practically inactivates the enzyme. The decrease in activity is about 40000-fold. Unexpectedly, elimination of the negative charge does not influence the ionization of the thiol group. Consequently, the reduction in activity is due to an adverse change in the position of the imidazole ring that is no longer able to fulfill properly its role as a general base catalyst.

REFERENCES

1. Krausslich, H.-G., and Wimmer, E. (1988) *Annu. Rev. Biochem. 57*, 701−754.
2. Skern, T., and Liebig, H.-D. (1994) *Methods Enzymol. 244*, 583−595.
3. Ryan, M. D., and Flint, M. (1997) *J. Gen. Virol. 78*, 699−723.
4. Bergmann, E. M., and James, M. N. G. (1999) in *Proteases of infectious agents* (Dunn, B. M., Ed.) pp 139−163, Academic Press, London.
5. Seipelt, J., Guarné, A., Bergmann, E., James, M., Sommergruber, W., Fita, I., and Skern, T. (1999) *Virus Res. 62*, 159−168.
6. Allaire, M., Cherney, M. M., Malcolm, A., and James, M. N. G. (1994) *Nature (London) 369*, 72−76.
7. Matthews, D. A., Smith, W. W., Ferre, R. A., Condon, B., Budahazi, G., Sisson, W., Villafranca, J. E., Janson, C. A., McElroy, H. E., Gribskov, C. L., and Worland, S. (1994) *Cell 77*, 761−771.
8. Mosimann, S. C., Cherney, M. M., Sia, S., Plotch, S., and James, M. N. G. (1997) *J. Mol. Biol. 273*, 1032−1047.
9. Sárkány, Z., Szeltner, Z., and Polgár, L. (2001) *Biochemistry 40*, 10601−10606.
10. Ivanoff, L. A., Towatari, T., Ray, J., Korant, B. D., and Petteway, S. R. (1986) *Proc. Natl. Acad. Sci. U.S.A. 83*, 5392−5396.
11. Cheah, K.-C., Leong, L. E.-C., and Porter, A. G. (1990) *J. Biol. Chem. 265*, 7180−7187.

12. Kean, K. M., Howell, M. T., Grünert, S., Girard, M., and Jackson, R. J. (1993) *Virology 194*, 360−364.
13. Hämmerle, T., Hellen, C. U. T., and Wimmer, E. (1993) *J. Biol. Chem. 266*, 5412−5416.
14. Nicklin, M. J. H., Harris, K. S., Pallai, P. V., and Wimmer, E. (1988) *J. Virol. 62*, 4586−4593.
15. Leatherbarrow, R. J. (1998) *GraFit, Version 4*, Erythacus Software Ltd., Staines, U.K.
16. Polgár, L. (1974) *FEBS Lett. 38*, 187−190.
17. Glasoe, P. K., and Long, F. A. (1960) *J. Phys. Chem. 64*, 188−190.
18. Polgár, L., Erdélyi, F., Hajnal, É., Löw, M., Gráf, L., and Korant, B. D. (1993) *Biochem. J. 290*, 797−800.
19. Polgár, L. (1989) *Mechanisms of Protease Action*, pp 87−122, CRC Press, Boca Raton, FL.
20. Vindigni, A., and Di Cera, E. (1996) *Biochemistry 35*, 4417−4426.
21. Ayala, Y. M., and Di Cera, E. (2000) *Protein Sci. 9*, 1589−1593.
22. Cleland, W. W. (1977) *Adv. Enzymol. Relat. Areas Mol. Biol. 45*, 273−387.
23. Schowen, K. B., and Schowen, R. L. (1982) *Methods Enzymol. 87*, 551−606.
24. Pallai, P. V., Burkhardt, F., Shoog, M., Schreiner, K., Bax, P., Cohen, K. A., Hansen, G., Palladino, D. E., Harris, K. S., Nicklin, M. J., and Wimmer, E. (1989) *J. Biol. Chem. 264*, 9738−9741.
25. Weidner, J. R., and Dunn, B. M. (1991) *Arch. Biochem. Biophys. 286*, 402−408.
26. Ellman, G. L. (1959) *Arch. Biochem. Biophys. 82*, 70−77.

BI027004W